Offprint from

Proceedings of the 15th International Symposium on

# Rarefied Gas Dynamics

June 16-20, 1986 Grado, Italy

## Volume II

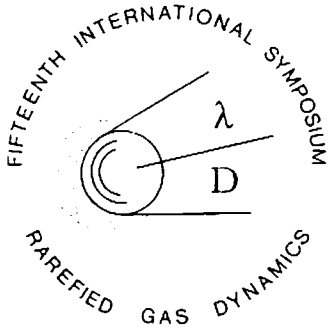


Edited by
Prof. Dr. Vinicio Boffi, University of Bologna, Italy
Prof. Dr. Carlo Cercignani, University of Milano, Italy

**B. G. Teubner Stuttgart 1986**

# COLLISION ENERGIES OF HEAVY SPECIES SEEDED IN SUPERSONIC $H_2$ JETS IMPINGING ON SURFACES AT LARGE BACKGROUND PRESSURES.

J. Fernandez de la Mora, P. Riesco-Chueca, R. Fernandez-Feria and J.B. Fenn, Yale University;*
J.J. Schmitt, Schmitt Technologies Associates, Science Park; New Haven, CT. 06520, USA

## 1. Introduction

Because seeded supersonic free jets can supply energetic beams of heavy molecules with translational energies of tens of eV[1], their applications have been numerous, principally under conditions where the source gas expands into a highly evacuated region where gas-gas or gas-surface interactions can occur under free-molecule conditions. Yet, recent work has shown that highly energetic heavy molecule-surface impacts can also be attained at jet densities such that the He or a $H_2$ carrier gas is in the continuum regime and thus forms a bow shock wave upstream of the target surface [6]. The heavy seed species, on the other hand, have sufficient inertia to penetrate through the low-speed shock layer of light fluid and collide with the surface at a large fraction of their pre-shock velocity. These high density conditions offer the substantial advantage of yielding molecular flux intensities at the surface that are orders of magnitude greater than can be obtained under true free molecule condition while still providing surface collision energies that can reach many eV for seed species of high molecular weight. Furthermore, because the background pressures need not be so low, the pumping speed requirements are relatively modest and can be met with ordinary rotary mechanical pumps[6]. However, the conditions of impact in this high density mode of operation remain to be fully characterized. Clearly, at sufficiently high post-shock densities, the hydrodynamic interaction between the two gases may be sufficient to slow down the heavy species and increase their velocity spread. Therefore, in order to make intelligent use of seeded jets as high-intensity sources of energetic neutral particles for gas-surface interaction studies, we wish to characterize the density dependence of impingement energy for the heavy species.

We shall first provide an approximate picture of the process of acceleration and post-shock deceleration that makes possible the calculation of impact energies as a function of the governing parameters. Then we will report experimental results on the impact-activated suface reaction of $W(CO)_6$ seeded in $H_2$ jets [5]. Such measurements embody a chemical velocimetry methodology by which reaction rates may be converted into impingement speeds, which compare favorably with the predictions of the model.

## 2. Impingement dynamics of free jet molecules on surfaces

We consider the expansion of a gas from a source at a stagnation pressure $p_0$ through a converging nozzle into a region at a backgrcund pressure $p_1$. At sufficiently high values of $\Pi=p_0/p_1$, the resulting jet has a structure comprising an isentropic core of supersonic flow surrounded by barrel-shaped lateral shock waves. The "bottom of the barrel" is formed by an intersecting shock pattern that takes the form of a normal shock wave, often refered to as a Mach disk. The distance along the jet-axis (z) where the Mach disk is encountered ($z_m$) is given by the empirical relation [2]:

$$R_m = z_m/d_n = 0.67\ \Pi^{1/2}, \qquad (1)$$

$d_n$ being the nozzle diameter. When the jet is intercepted by an infinite flat surface, two possible effects can be observed. If the plate is at a distance from the nozzle exit $z_p$ sufficiently larger than $z_m$, the location of the Mach disk remains unchanged. However, if the surface is closer than $z_m$, the Mach disk is replaced by a normal shock wave some distance ahead of the surface[11]. The relevant parameter is therefore the ratio $\zeta = z_p/z_m$, where $z_p$ is the nozzle-to-plate distance and $z_m$ is the distance from the nozzle exit to the location of the Mach disk in the absence of the surface,

$$\zeta = z_p/z_m. \qquad (2)$$

Between the shock and the wall there is a nearly incompressible subsonic shock layer of thickness e which, for a strong shock and a velocity field varying linearly with position, may be shown to be:

$$e/z_p = (\gamma - 1)/2(\gamma + 1), \quad (3)$$

where $\gamma$ is the specific heat ratio $c_p/c_v$ of the gas. Experimental data in air($\gamma = 1.4$) show that Eq.(3) holds for all combinations of $z_p$ and $\Pi$ provided that $\zeta < 0.6$ [6]. In this case, the flow close to the centerline can be divided into two regions: an isentropic expansion where the gas, after leaving the nozzle, accelerates to velocities close to the terminal speed $V_\infty = [2\gamma T_0 k/m(\gamma - 1)]^{1/2}$ (k is Boltzman's constant, m the molecular mass, and $T_0$ the source temperature), and a nearly incompressible post-shock region where the gas velocity is approximately linear with the distance to the wall.

To determine the impingement velocity of the heavy molecules we shall treat separately their behavior in the accelerating supersonic region and in the decelerating subsonic layer. We consider only the case when the heavy component is very dilute and does not affect the flow ofthe light gas.

2.1 Acceleration dynamics

The fluid discharging from a converging nozzle approaches a radial sorce flow near the axis at a distance of a few diameters from the nozzle. The observed far field flow can be approximated by a spherical expansion with virtual sonic conditions at a radius $r = \beta d_n$ where $\beta$=0.68 for monoatomic and 0.6 for diatomic gases [10]. Defining normalized variables for the light gas as

$$\eta = u/V_\infty \; ; \quad \theta = T/T_0 \; ; \quad R = r/d_n \, ,$$

sufficiently far from a converging nozzle (R > 2 , 3) and close to the jet-axis, the mass and energy conservation equations for the isentropic light gas take the following universal form [10]:

$$R^2 = \beta^2 [(\gamma+1)/2]^{-(\gamma + 1)/2(\gamma - 1)} [(\gamma-1)/2]^{1/2} \eta^{-1} \theta^{-1/(\gamma-1)} \quad (4)$$

$$\theta = 1 - \eta^2. \quad (5)$$

The problem of determining the velocity $u_p$ of the heavy gas has been considered by a number of authors [4]. Here, a more realistic drag law coupling the two gases is used [9]. Neglect of the stress tensor of the heavy gas in its momentum conservation equation (a hypersonic closure) yields for a spherical flow:

$$\tau u_p du_p/dr = v_B(u - u_p) \quad (6)$$

where $\tau$ is the relaxation time, related to the first approximation of the diffusion coefficient D given by the Chapman-Enskog theory for binary mixtures,

$$D(n + n_p)/n = kT\tau/m_p \; ; \quad (7)$$

n and $n_p$ are the number densities of the light and heavy gas, respectively, and $m_p$ is the molecular mass of the heavy gas. $v_B$ is a coefficient accounting for the nonlinearities of the drag law in the slip velocity $u-u_p$, and tending to unity as u tends to $u_p$ [9].

For sufficiently high values of the nozzle Reynolds number the heavy molecules become uncoupled from the suspending gas only in the supersonic region, where Eq.(4) holds true independently of the geometry of the converging nozzle. But Eq. (6) cannot be used in the transition region between nozzle and spherical flow, where u is generally not known and the flow is two-dimensional. However, if r is considered as a streamline coordinate, Eq. (6) determines the heavy gas near-axis velocity field provided that u(z) is completely specified. Given a nozzle geometry, the computation of u(z) in the subsonic region is rather demanding, involving the solution of a transonic problem. Furthermore, the nozzle shape affects the subsonic flow field and thus the final value of the velocity of the heavy gas whenever nonequilibrium effects set in within the

subsonic region. This matter is further discussed in Ref.[8], which also reports on experimental data for u(z) along the jet centerline for a few geometries. Our somewhat arbitrary choice for u(z) in this study is a parabolic function, corresponding roughly to a troncoconical nozzle, $u/u_0 = (1+z/d_\eta)^2$, where z takes negative values inside the nozzle ($-d_\eta$ at the inlet and zero at the exit). The sonic surface is assumed to coincide with the nozzle exit plane so that $u_0=u(M=1)$. For the transition region between the nozzle and the far field flow we assume the interpolation function: $R=R_1[dy+(1-d)y^e]$, where $R_1$ corresponds to a far-field starting point ($R_1=R(\eta=\eta_1=0.85)$ in Eq.4), $y=(\eta-\eta_0)/(\eta_1-\eta_0)$, with $\eta_0=u_0/V_\infty$ and $e=(d_1-d)/(1-d)$, where $d=d(R/R_1)/dy|_{y=0}$ and $d_1=d(R/R_1)/dy|_{y=1}$ in Eq(4).

Defining $\xi=u_p/V_\infty$, Eq. (6) becomes,

$$(\tau V_\infty/d_\eta)\xi d\xi/dR= \nu_B(\eta-\xi), \quad (8)$$

where $\tau$ and $\nu_B$ depend on $\rho$ and T. Eq. (8) is numerically integrated to yield the terminal heavy gas velocity $\xi_\infty = \xi(R\to\infty)$, shown in Fig.1 for the cases $\gamma$= 1.4 and $\gamma$=5/3 as a function of $S_a$ and $T_0^*$ where

$$T_0^* = kT_0/\varepsilon; \qquad S_a=T_0^{*1/3}m_p/(mn_0d_\eta\sigma^2). \quad (8')$$

$\varepsilon$ and $\sigma$ are the depth and location of the energy well for a Lennard-Jones interaction potential between the two different molecules. The choice of $S_a$ as a parameter is motivated by the low temperature limit of $\tau$ prevailing at large R, $\tau=0.080352m_pT^{*1/3}/[mn\sigma^2(kT/m)^{1/2}]$, based on which $S_a$ is related to the Stokes number of aerosol dynamics Stk, the ratio between $\tau$ at stagnation conditions and the fluid-dynamic time $d_\eta/(\gamma kT_0/m)^{1/2}$ characterizing the rate at which the process of acceleration occurs: $Stk= 0.080352\,\gamma^{1/2}\,S_a$.

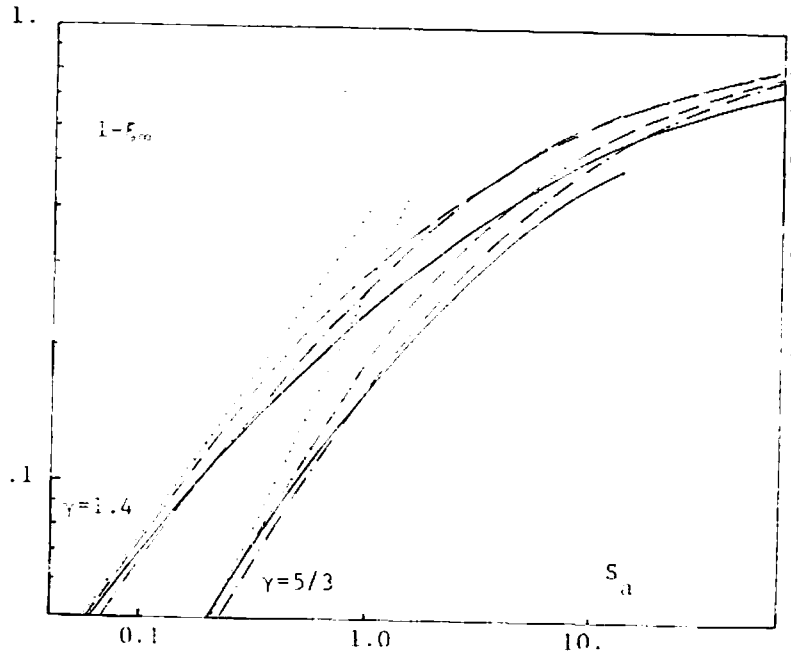


Fig.1: Terminal heavy-gas slip velocity $1-\xi_\infty$ as a function of $S_a$, and $T_0^*$ (Eq.8). $\gamma$=5/3 for the lower curves and 1.4 for the upper curves. The asymptotic behaviour at small $S_a$ (....) is given by Eqs.(10). Lines ——, - - -, and -·-·-, correspond to numerical results for values of $T_0^*$ of 100,10 and 1.

Eq. (8) can be cast into phase plane form by combination with Eq. (4) to yield:

$$S_a \xi d\xi/d\eta = C_a \eta^{-3/2} \theta^{-1/12} (4\eta^2 - 1)(\eta - \xi) \nu_B \qquad (9a)$$

with Ca=1.0784 for monoatomic gases, and

$$S_a \xi d\xi/d\eta = C_a \eta^{-3/2} \theta^{5/12} (6\eta^2 - 1)(\eta - \xi) \nu_B \qquad (9b)$$

with $C_a$ = 0.733055 for diatomic gases. A singular perturbation scheme close to the point $\eta$=1 ignoring nonlinear corrections ($\nu_B$ = 1) yields for small values of $S_a$:

$$1 - \xi_\infty = 0.279\ S_a^{12/11} \quad (\gamma = 5/3) \qquad (10a)$$

$$1 - \xi_\infty = 0.3793\ S_a^{12/17} \quad (\gamma = 1.4). \qquad (10b)$$

Eqs. (10) are plotted in Fig. 1 together with the numerical results for various values of $T_0^*$, showing good agreement for small values of $S_a$. Fig. 2 shows the evolution of the mean heavy gas velocity as a function of R for two values of $S_a$ ($T_0^*$=1, $\gamma$= 1.4 and 5/3). It can be observed that the terminal speed is reached only a few diameters away from the nozzle.

2.2 Deceleration dynamics

The heavy component, penetrating in the shock layer in front of the intercepting obstacle, experiences a deceleration which can be strong enough to bring its normal velocity to zero before it hits the surface. Yet, under favorable conditions, the heavy species may also encounter the obstacle with a finite mean speed which we wish now to evaluate.

Let $\eta$, $\zeta$, $\theta$ be defined as above and let e be the shock stand-off distance in the region close to the centerline, where the flow is one-dimensional and the shock wave is normal. The following assumptions are introduced: the light gas velocity before the shock is approximated as the terminal speed ($\eta$ =1), which is accurate even a few nozzle diameters away from the source. Therefore the upstream Mach number is high and the strong-shock jump relations can be used. A quantitative criterion for the range of validity of these assumptions can be derived from Eq. (4). The light gas compression in the shock wave is independent of the heavy molecules; the thickness of the shock and the wall bondary layer are small under typical conditions, leading to small corrections that we incorporate later on. Based on the small thickness of the shock layer and on the good agreement between its observed thickness and that of Eq. (3), the light gas flow is assumed to be incompressible and such that $\eta$ decreases linearly from its post-shock value to zero within the subsonic region, so that, in terms of the normalized coordinate

$x = (z - z_S)/(z_p - z_S)$, $\eta$ is given by $\eta = \delta(1 - x)$,

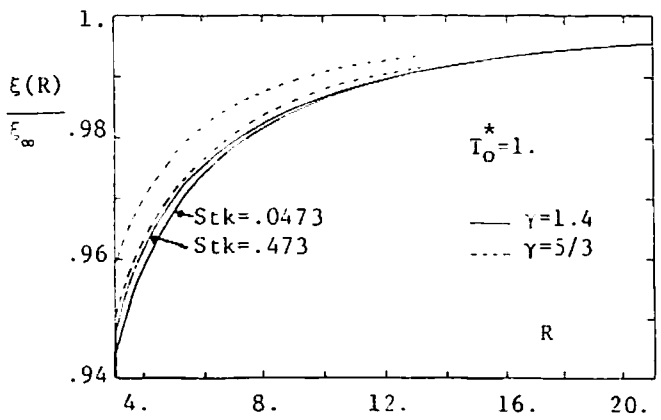


Fig.2:
Evolution of the velocity $\xi$ of the heavy gas in the free jet as a function of the distance to the nozzle $R=z/d_n$. For $\gamma$=1.4 (——), $\xi$(R) depends negligibly on the source pressure (Stk) over the full experimental range

where $\delta=(\gamma-1)/(\gamma+1)$ is the strong-shock density ratio. The relaxation equation becomes

$$S_d\,\xi\,d\xi/dx = v_B(\eta-\xi) \qquad (11)$$

with $S_d = \tau_2 V_\infty/e$, while $\tau_2$ is based on post shock stagnation conditions. Eq.(11) is complemented with the boundary condition $\xi=\xi_0$ at $x = 0$, where $\xi_0$ is the pre-shock heavy gas velocity obtained from the calculations of the previous section. In the relevant high temperature limit, Eq.(11) can be written as:

$$S_d\xi d\xi/dx=[1+B(\xi-\eta)^2]^{1/3}(\eta-\xi) \qquad (12)$$

with $B = 1.149$ and $S_d = 0.2945\, m_p T_0^{*1/6}/(mn_0 e\sigma^2)$. The light gas temperature in the shock layer is asumed uniformly equal to the stagnation temperature $T_o$. The variables $T_0^*$ and $\sigma$ are defined as in Eq. (8).

The numerically integrated $\xi_w = \xi(x=1)$ as a function of $S_d$ is represented in Fig. 3 for different values of $\xi_0$, together with a linear approximation $\xi_{wL}$ resulting from seting $v_B=1$. Although this method overestimates $\xi_w$, the absolute errors are less than 4% for the most unfavorable case when $\xi_0=1$, and become negligible when $\xi_0 \le 0.6$. A phase-plane analysis shows that a non zero impaction velocity ($\xi_{wL} > 0$) exists when $S_d > 1$ for $\xi_0 < 1/2$, or when $Sd > (1 - 1/4\xi_0)/\xi_0$ for $\xi_0 > 1/2$ ($\gamma=5/3$, monoatomic gas). The resulting values for $\xi_{wL}$ are:

$$\xi_{wL}= [\xi_0^2-(\xi_0-1/4)/S_d]^{1/2}\exp\{-(S_d-1)^{-1/2}\tan^{-1}[(S_d-1)^{1/2}/(2S_d\xi_o-1)]\},\quad S_d>1\ ;$$
$$\xi_{wL}= [\xi_0^2-\xi_0-1/4)/S_d]^{1/2}\{[2S_d\xi_0-1-(1-S_d)^{1/2}]/[2S_d\xi_0-1+(1-S_d)^{1/2}]\}^{1/[2\sqrt{(1-S_d)}]},$$
$$(1-1/4\xi_0)/\xi_0 < S_d < 1;\ \xi_0 < 1/2\ . \qquad (13)$$

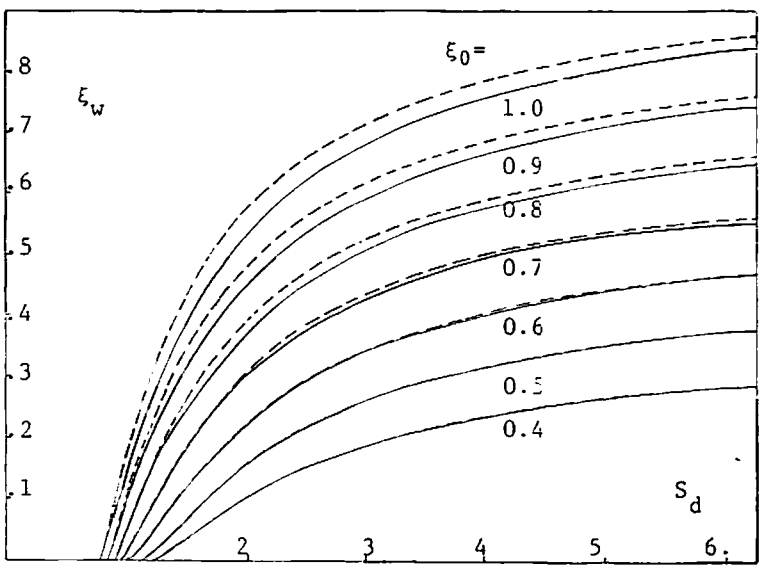


Fig.3:
Velocity retained by the heavy gas after crossing the shock layer as a function of the pre-shock velocity $\xi_0$ and $S_d$ (Eq.12). ——, numerical solution of Eq.12. - - -, analitical results (Eq.13) for a linear drag law ($v_B=1$), which provide an accurate prediction when $\xi_0 \le 0.6$.

2.3 Viscous effects

The effect of the viscous boundary layer at the impact surface may be accounted for approximately by adding a stagnant region of thickness $e_v$ near the wall, with

$$e_v/e = 0.804\ \{\nu/[\delta V_\infty e]\}^{1/2}, \qquad (14)$$

where $\nu$ is the kinematic viscosity $\mu/\rho$ of the light gas at post-shock stagnation conditions. Additional use of the linear drag law ($\nu_B = 1$) results in a velocity loss equal to $e_v/\tau_2$, which, for the case of $H_2$-$W(CO)_6$ mixtures with an estimated value of the Schmidt number ($Sc \equiv \nu/D$) of 3, leads to the relatively small reduction in impact speed $\Delta\xi_w$

$$\Delta\xi_w = 0.0793\ S_d^{-1/2}\ . \qquad (15)$$

Additional viscous effects due to the finite width $e_s$ of the shock wave, are inversely proportional to the same Reynolds number entering into Eq. (14), $e_s/e \sim \nu/(\delta V_\infty e)$, and will be neglected here.

## 3 Experimental work

In the following experiments we infer the values of the impingement speeds $\xi_w$ from impact-activated reaction probabilities of $W(C0)_6$ seeded in $H_2$ beams first observed by Connolly et al.[5]. The main operating parameters are $p_0/p_1 = \Pi \simeq 3400$ and $292K < T_0 < 299K$.

Figure 4 shows a sketch of the experimental apparatus used, a slight variation of the one described in Ref.[6]. Hydrogen from a tank flows through a regulating valve to reach a source pressure $p_0$. It then passes through a cell containing $W(CO)_6$ crystals, and then reaches the nozzle. The heavy vapor entrained with the $H_2$ gas is not completely saturated, but its concentration is measured by passing the mixture through an atomic absorption Hg analyzer (Coleman 50). Many metal carbonyls absorb strongly in the region around 250 nm [7], and the Coleman analyzer yields a linear response some 30 times smaller at room temperature for saturated $W(CO)_6$ than for saturated Hg. For our system, the degree of saturation Sat of the carbonyl vapor achieved by passing the hydrogen through the cell varied approximately linearly with the cell pressure (the source pressure $p_0$) as $Sat=1\text{-}6.25\ 10^{-4}\ torr^{-1}\ p_0$.

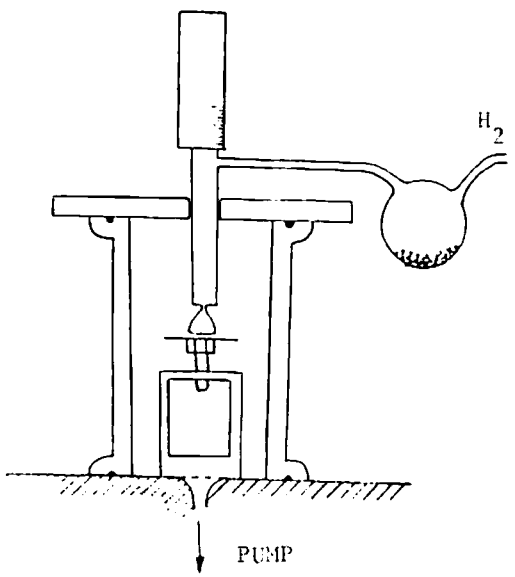


Fig.4
Sketch of theapparatus.

After the cell , the gas expands through a converging sapphire nozzle, accurately shaped as a truncated cone (1.75 mm basis diameter; 60°semiangle) ending on a 0.21 mm cylinder 0.13 mm in diameter. Facing the jet perpendicularly is a 1.8x1.8 cm glass slide

supported on a rod whose movement is controlled by a micrometer drive with a precision on the order of 0.025 mm. The target is housed in a downstream chamber evacuated by an oil rotary pump (Balzers) capable of producing a background pressure $p_1$ 3400 times smaller than the source pressure $p_0$ when $H_2$ gas at room temperature flows through the nozzle (0.13 mm in diameter) at high Reynolds numbers. The downstream pressure $p_1$ is measured with an MKS barotron gauge and spans the range between 0.02 torr and 0.6 torr. Upstream pressures are measured with a mercury manometer in the range between 60 torr (below which no reaction occurs) and near one atmosphere. Nozzle to plate distances range from 3 to 28 nozzle diameters ($0.076 \leq \zeta \leq 0.72$).

The experimental information that we report relate to the products of impact activated reaction left on the glass slide. Connolly et al [5] have shown that $W(CO)_6$ seeded in $H_2$ jets decomposes upon sufficiently energetic surface impacts, with a rate of reaction increasing sharply above a threshold speed which they estimated to be 1.7 Km/s. The product of decomposition remains on the surface as a nearly involatile solid and is sufficiently transparent to show several dark interference (Newton's) rings, from which the shape and volume of the deposit may be inferred [6]. If $\lambda$ is the wavelength of the light used to observe the interference fringes and n the index of refraction of the condensate, the mth dark outward ring reveals a deposit of heigth $m\lambda/2n$. Results for $z_p=16d_n$ are shown in Fig.5, obtained by means of two different filters with maximal transmissions centered at 630 and 525 nm.

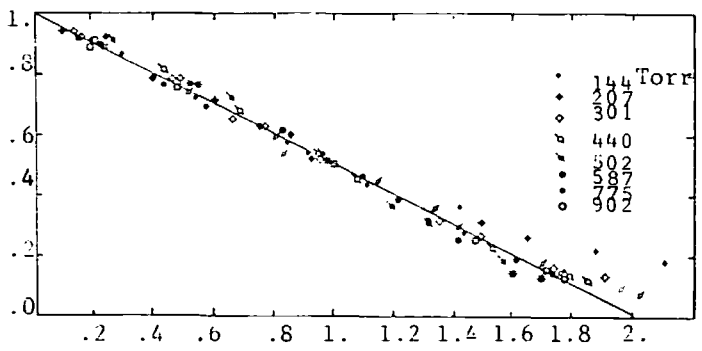


Fig.5: Normalized heigth of the reacted $W(CO)_6$ as a function of the squared radial variable found from light interference patterns. Nozzle to plate distance $z_p/d_n$= 16. Notice that the curve is close to a parabola with a wing that decreases at increasing pressures.

The plot shows the ring number m (the height normalized by $\lambda/2n$ with $\lambda$=525 nm) vs the square of r, its radius. Except for a small wing that becomes fainter above a pressure of 200 torr, these thin films have a shape roughly parabolic which we characterize by means of their maximum height $m_0' \equiv dm/dt$ (rings/minute) and the width parameter $d_{1/2}$, or twice the radial position where the deposit height is one-half of the maximum. We shall measure the reaction rate in terms of the optical volume V formed per unit time, given roughly by

$$V \equiv \pi m_0' d_{\zeta}^2/4 . \qquad (16)$$

Figure 6a shows raw data on the optical volume per unit time V deposited as a function of the nozzle-to-plate distance $z_p$ for a variety of source pressures. An asymptote is approached as $z_p/d_n > 16$, indicating proximity to free-molecular conditions, with only slight decelerating effects of the plate on the heavy gas. At decreasing values of $z_p$ the post-shock pressure increases (smaller values of $S_d$) and the corresponding loss in heavy-molecule impact velocities is seen as a relatively sharp decrease in V.

Because the kinetic energy of translation is much greater than those associated with the internal thermal energy of the molecule or the surface, it may be asumed that the reaction probability depends only on the speed of impact $\xi_w$ [6]: $V=V(\xi_w)$. Knowledge of this function would make it

possible to convert the $V(p_o,z_n/d_n)$ curves of Fig.6a into the form $\xi_w=\xi_w(p_o,z_n/d_n)$, which could be used to test the validity of the previous theoretical model. Alternatively, because two degrees of freedom are available in our experiments, one may be used to determine the kinetic curve $V(\xi_w)$, while still another is left to check the validity of the above method of computing $\xi_w$. The success of such an approach is illustrated in Fig.6b, where reduced experimental values of V are represented as a function of the value of $\xi_w$ computed for every condition of source pressure and nozzle to plate distance.

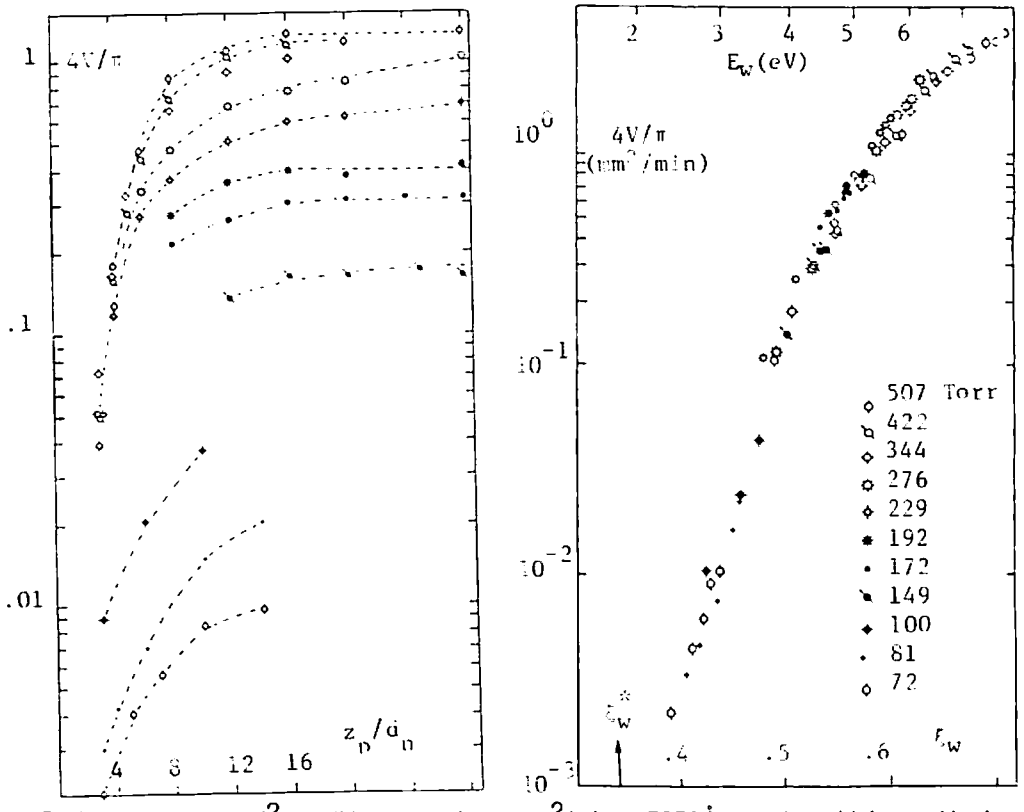


Fig.6: Optical volume $m'_o d^2_{1/2}$ (Newton's rings $mm^2$/min at 5250Å wavelength) formed by impact of $W(CO)_6$-$H_2$ jets on glass slides. (a) Raw data for a variety of source pressures and nozzle to plate distances $z_p/d_n$. (b) same data as in (a) corrected for incomplete saturation of the $W(CO)_6$, and refered to "standard" conditions based on the vapor pressure of the carbonyl at 299 K. The abcissa is the impact velocity $\xi_w$ calculated from the experimental conditions as explained in section 2.

No free parameters are available in the above conversion. V has been corrected for the incomplete and pressure dependent degree of saturation of the $W(CO)_6$ vapors through division by the group $Sat= 1-6.2510^{-4}$ $torr^{-1}$ $p_o$, determined experimentally. It is also multiplied by the ratio of the known[3] vapor pressure $p_v$ of $W(CO)_6$ at 299 K over its value at the cell temperature. For the determination of $\xi_w$ we first convert the source pressure into the variable $S_a$ (approximately equal to $0.65\,\gamma^{1/2}p_o$, with $p_o$ in atm), and extract the value of $\xi_\infty$ from Fig.1. Use of Fig.2 yields the carbonyl speed $\xi_o$ at the head of the shock. Entering with the values of $S_d$ (resulting from Eq.45

of Ref[6]: $S_d$=20.417Stk $z_p/d_n$) and $\xi_o$ in Fig.3 (or into Eq.13 when $\xi_o \leq 0.6$) yields $\xi_w$ uncorrected for viscous effects, while Eq.15 leads to the final prediction for the value of $\xi_w$ used to construct Fig.6b.

In light of the variety of approximations involved in the determination of $\xi_w$, it is quite remarkable to see that the many families of curves of Fig.6a have collapsed into a single curve with a scatter of only around 2% of the terminal speed. This result is the more surprising when one realizes that the rotational degree of freedom of $H_2$ is not completely in equilibrium so that $\gamma$ cannot be taken exactly as 1.4[6]. Nonetheless, this fact would lead to a maximum variation of 18% in the terminal velocity of the light gas, with a much smaller effect under our conditions, where the nozzle Reynolds number is in the range 100-1000.

For the determination of $\xi_w$ we have taken $\gamma$=1.4 through the acceleration process, and $\gamma$=5/3 for the post-shock deceleration. Because the former approximation is probably the weakest link in the chain of arguments leading to $\xi_w$, we attempted to run these experiments with He as the carrier gas. Unfortunately, we have not succeeded in observing any reaction with such jets, even under conditions where the target was a thin cylinder with a negligible stoping power, and the resulting impingement energies were above 2.5 eV. Because collisions at such energies would activate the reaction when $H_2$ is the carrier gas, one could speculate that $H_2$ plays an active role in the surface chemistry. However, the work of Connolly et al.[5] and Fig.6b indicate that the reaction is independent of the background pressure of $H_2$, at least down to very small partial pressures.

Aside from lending strong support to our previous theoretical considerations, the collapse of the data points of Fig.6a into the single curve of Fig.6b yields a reasonably reliable description of the kinetics of the reaction process. To provide a system-independent, universal result, the coordinate V should be further normalized by the nozzle area, while the $\xi_w$ variable has to be converted into an absolute energy scale, as done in the figure ($E_w$=15.6 $\xi_w^2$ eV). Data on the unknown values of the density $\rho_s$ and refractive index n of the deposit would allow converting the optical volume V into actual deposited mass, and thus into an absolute "reaction probability" P. Nonetheless, based on the values $\rho_{os}$=10 gr cm$^{-3}$ and $n_o$=1, we may define the modified (but known) reaction probability P'

$$P' = n P \rho_{os}/\rho_s,$$

which differs from P by an unknown factor of order one, and which for our value of $d_n$=0.13 mm, is related to the variable $4V/\pi$ of Fig.6b through the constant A=4.82 10$^{-3}$ mm$^{-2}$ min:

$$P' = A m_o' d_{1/2}^2.$$

The maximum value of P' in Fig.6b is thus only 2%. Our previous conclusion on reaction probabilities of order one [6] was in error by a factor $m_p/2m$ and must be abandoned.

Fig.6b shows also the value $\xi^*_w$=0.342 corresponding to the known W-C bond energy of 42.1 Kcal/mole [3], quite close to our lowest data point at $\xi_w$=0.39 where, although P'=10$^{-5}$, the reaction rate is still substantial and could be measured accurately with a collection time of only 15 minutes. Notice also that sonic conditions for $H_2$ correspond to $\xi_w$ =0.408, so that subsonic velocities are not incompatible with a fair rate of reaction. We have directly reconfirmed this point by observing the decomposition of $W(CO)_6$ by impact on thin cylinders placed right at the (sonic) exit of a larger conical nozzle with a throat diameter of 0.75mm. This result demands a revision of the previously reported threshold velocity, estimated in the pioneering work of Connolly et al. [5] to be around 1.7 Km/s ($\xi_w$=0.576). Considering that the threshold value of $\xi_w$ is unambiguously bracketed in the narrow interval 0.342< $\xi_w \leq$ 0.408, it is probable that the minimum translational energy required to activate the reaction will fall close to the W-C bond energy of 42.1 Kcal/mole.

Notice also that our prediction for $\xi_W$ is most likely an upper limit for the actual value, because nonequilibrium effects in the expansion of $H_2$ result in a smaller terminal speed of the carrier gas. Because rotational nonequilibrium effects are highest at the smallest source pressures, the larger inaccuracy in the model occurs at the lowest point in Fig.6b ($\xi_W$=0.39). But the real value of $\xi_W$ corresponding to this point must be between the upper bound 0.39 and the lower bound 0.342 below which no reaction can possibly occur. The range left for errors in our most inaccurate point is thus rather narrow, and will shrink further in planed reactive experiments at still smaller values of $\xi_W$. As a final remark on the peculiar properties of the jets studied, notice the lowest point corresponding to a source pressure of 507 torr: The impact energy is 3.75 eV with a plate only 3 nozzle diameters away from the source. The same conditions could have been attained with a pressure ratio of 56 and 9 torr of background pressure.

In conclusion, this work provides a method of computing impingement energies of heavy seeded species under conditions of strong hydrodynamic interaction with the target, as well as an indirect determination of the kinetics of the impact-activated surface decomposition of $H_2$-$W(CO)_6$ jets. Although not completely unambiguous, these results have passed successfully several stringent self-consistency checks, and may thus be taken as fairly reliable.

This work has been supported by a Cooperative Research Grant (number 85-176) from the State of Connecticut and Schmitt Technologies Associates.

References

[1] J.B Anderson, R.P. Andres and J.B. Fenn, in Advances in Chemical Physics, vol X, Edited by J Ross, Interscience, 1966.
[2] W. Ashkenas and F.S. Sherman, in Rarefied Gas Dynamics, J.H. de Leeuw, editor, Academic Press, New York, 1966.
[3] F. Calderazzo, E. Ercoli, and G. Natta, in Organic Synthesis via Metal Carbonyls, Edited By I. Wender and P. Pino, Interscience Publishers, New York, 1968.
[4] R.Cattolica, R.J. Gallagher, J.B. Anderson and L. Talbot, AIAA J.,17,344,1979.
[5] M.S. Connolly, E.F. Greene, C. Gupta, P. Marzuk, T.H. Morton, C. Parks and C. Staker, J. Phys. Chem.,85,235-240,1981.
[6] J. Fernandez de la Mora, J.Chem. Phys., 82,3453,1985.
[7] R.T. Lundquist and M. Cais, J. Organic Chem.,27,1167,1962.
[8] H. Murphy and D. Miller, J. Phys. Chem.,88,4474,1984.
[9] P. Riesco-Chueca, R. Fernandez-Feria, and J. Fernandez de la Mora, this Symposium,1986.
[10] F.S. Sherman, in Rarefied Gas Dynamics, J.A. Laurmann, editor, Vol II, pp228-60,1963.
[11] R.R. Vick and E.H. Andrews, Jr., NASA TN D-3269,1966.

(*)Department of Mechanical Engineering, P.O. Box 2159 Y.S. New Haven, CT. 06520, USA.